

X-ray - Infrared relation of AGNs and search for highly obscured accretion in the *AKARI* NEP Field

Takamitsu Miyaji^{ID} and *AKARI* NEP Survey Team

Instituto de Astronomía, Universidad Nacional Autónoma de México, Km. 103 Carret.
Tijuana-Ensenada, Ensenada, 22860 Mexico
email: miyaji@astro.unam.mx

Abstract. The infrared Astronomical Satellite *AKARI* conducted deep ($\sim 0.4 \text{ deg}^2$) and wide ($\sim 5.4 \text{ deg}^2$) surveys around the North Ecliptic Pole (NEP) with its InfraRed Camera (IRC) with nine filters continuously covering the $2\text{--}25 \mu\text{m}$ range. These photometric bands include three filters that fill the “*Spitzer* gap” between the wavelength coverages of IRAC and MIPS. This unique feature has enabled us to make sensitive mid-infrared detection of AGN candidates at $z \sim 1\text{--}2$, based on the Spectral Energy Distribution (SED) fitting including hot dust emission in the AGN torus. This enables us to compare X-rays and the AGN torus component of the infrared emission to help us identify highly absorbed AGNs, including Compton-thick ones. We report our results of the *Chandra* observation of the *AKARI* NEP Deep Field and discuss the prospects for upcoming *Spectrum-RG* (eROSITA+ART-XC) on the *AKARI* Wide field.

Keywords. galaxies: active – infrared: galaxies – X-rays: galaxies

1. Introduction

There are three major bumps in the electromagnetic continuum in a typical AGN: 1) optically-thick thermal emission from the accretion disk in the ultraviolet, 2) the primary X-ray continuum by the inverse-Compton scattering of the disk ultraviolet photons by hot coronae, and 3) the infrared emission from hot dust in the circum-nuclear torus. Additionally, reprocessed primary X-ray continuum by reflections at surrounding material produces a characteristic “Compton hump” in hard X-rays. Observational determination of how these three components are inter-related is a key to panchromatic modelings of the AGN component in galaxies.

In multiwavelength extragalactic surveys, X-rays are considered the most efficient marker of the AGN activity. However it is subject to absorption by intervening gas by photo-electric absorption, which occurs mainly at photon energies $E < 10 \text{ keV}$. If the line of sight column density becomes $N_{\text{H}} \gtrsim 10^{24} \text{ cm}^{-2}$, the effects Compton scattering further attenuates X-ray emission even at $E \gtrsim 10 \text{ keV}$.

While the infrared emission from hot dust heated by AGNs is less subject to absorption by intervening material, it has to be separated from stars and warm dust from star-formation regions by an SED decomposition to measure the IR luminosity of the AGN component alone.

The continuous 9-band $2\text{--}25 \mu\text{m}$ photometric data available from *AKARI* NEP Survey are ideal for such SED decomposition of galaxies. The availability of three photometric bands in the $11\text{--}20 \mu\text{m}$ range, which is the wavelength gap between IRAC and MIPS instruments of *Spitzer*, makes the *AKARI* IRC dataset a very strong tool for

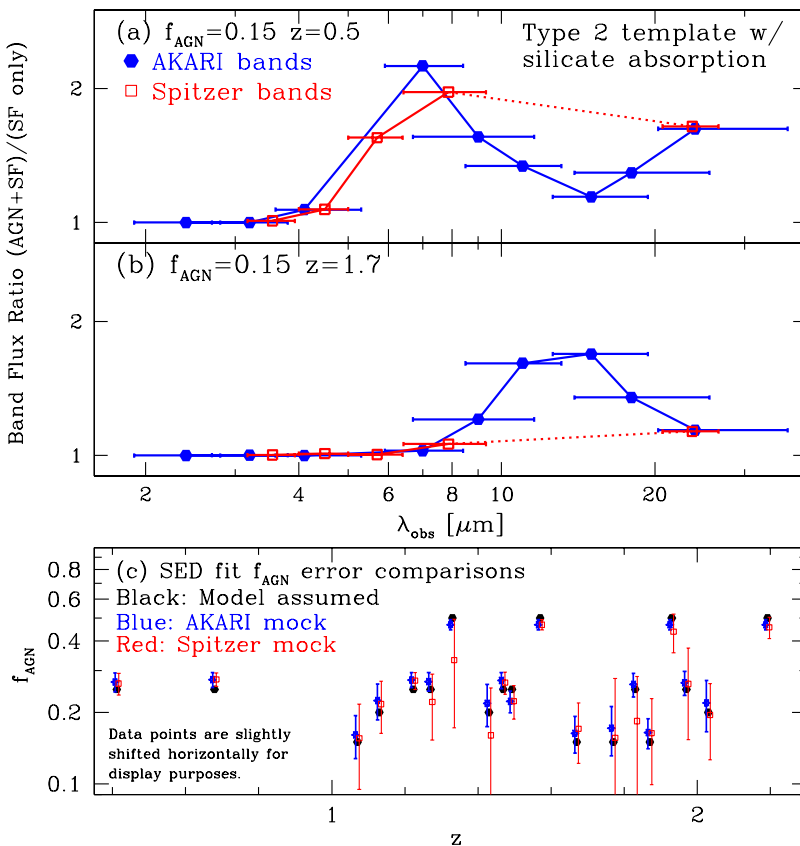


Figure 1. (a) & (b): Excess MIR emission ([AGN+Starburst]/Starburst), due to the presence of a type 2 AGN (with the 9.7 μm silicate absorption feature) observed through the *AKARI* IRC (blue/filled hexagon) and *Spitzer* IRAC+MIPS (red/open square) filter sets, for (a) $z = 0.5$ and (b) $z = 1.7$ objects. An AGN fraction $f_{\text{AGN}} = 0.15$ of the total IR luminosity is assumed. (c): Comparisons of expected f_{AGN} errors between SED fits to a number of simulated SEDs (black/filled symbol without error bars) through *AKARI+Herschel* (blue/filled symbol with error bars) and *Spitzer+Herschel* (red/open square with error bars). In calculating the errors, imaging depths of ANEPD and COSMOS are assumed for the former and the latter respectively. The calculations are made by the Cigale software using the model in Ciesla *et al.* (2015).

separating AGN hot dust emission from stellar+star-formation components at $1 \lesssim z \leqslant 2$ (the “Cosmic Noon”).

In this proceedings article, we summarize the results and prospects of our X-ray followup studies of the *AKARI* NEP field with emphasis on X-ray data and the connection between X-rays and infrared. These include our *Chandra* followup studies of the *AKARI* NEP Deep Field and prospects of upcoming *Spectrum-RG* (eROSITA+ART-XC) observations.

2. The *AKARI* NEP Survey

AKARI was a Japanese IR astronomical satellite (Matsuura *et al.* 2006; see also Goto *et al.*, this symposium), which was operated from 2006 to 2011. One of the unique features of the observatory was the availability of continuous wavelength coverage over 2–25 μm in 9 filters with its IR Camera (IRC), including three filters in the 11–19 μm range. These filters fill the 9–20 μm gap between the *Spitzer* IRAC and MIPS instruments and

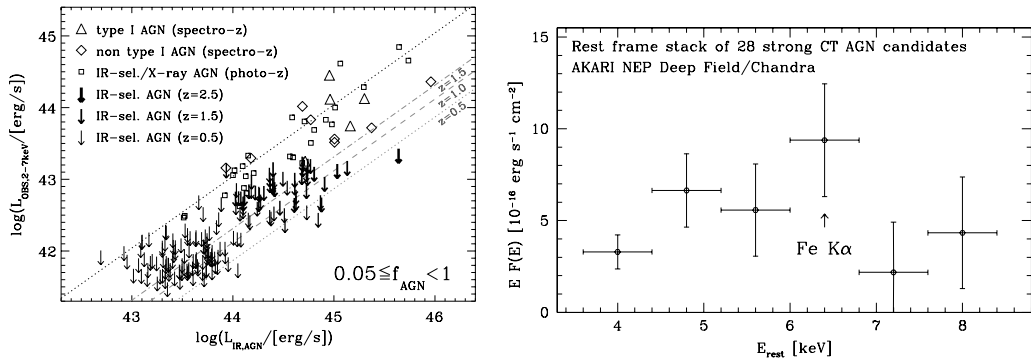


Figure 2. *Left:* Infrared AGN rest-frame luminosity from SED fits vs. hard (2–7 keV) observed X-ray luminosity. The symbols represent: triangles – spectroscopically-confirmed type I AGNs, diamonds – objects with optical spectra that do not show broad emission lines, small squares – IR-selected AGN that are also detected in the 2–7 keV band with photometric redshifts only, downward arrows – IR-selected AGN undetected 2–7 keV band, where the vertical position corresponds to the 2–7 keV flux upper limit. The thickness of the arrows represents the redshift of the source. The dotted line shows the correlation between the AGN IR luminosity and the X-ray luminosity ($\langle L_{\text{X}}/L_{\text{IR}} \rangle = 0.11$) for unabsorbed AGNs. The gray lines show for different redshifts the expected attenuation of the 2–7 keV X-ray luminosity caused by an intrinsic absorption of $N_{\text{H}} = 10^{24} \text{ cm}^{-2}$. Adopted from K15 (Fig. 18). *Right:* The rest-frame stacked spectrum of the 28 strong CT AGN candidates calculated using the CSTACK utility.

allows an efficient selection of AGN at $1 \lesssim z \lesssim 2$ in the MIR. This redshift range (the so-called Cosmic Noon) is particularly important to study since that is where both the X-ray detected number and luminosity densities peak.

Figure 1 demonstrates the advantage of the continuous wavelength coverage of *AKARI* 9-band photometry (including 10–19 μm) over the *Spitzer* IRAC+MIPS photometric bands in detecting the AGN torus component. (See caption.)

As a legacy program of *AKARI*, a major portion of all pointed observations during its liquid helium phase was devoted to surveys around North Ecliptic Pole (NEP), namely the AKARI NEP Deep ($\sim 0.4 \text{ deg}^2$; hereafter ANEPD) and Wide ($\sim 5.4 \text{ deg}^2$; ANEPW) field surveys with IRC. At ANEPD, the *AKARI* data have 5σ sensitivity limits of, e.g., ~ 9 and $87 \mu\text{Jy}$ at 3.2 and 15 μm respectively (Murata *et al.* 2013), while the limiting fluxes are approximately twice as large in NEPW (Kim *et al.* 2012).

3. Chandra Observations of the *AKARI* NEP Deep Field

We were granted a 250 ks dense tiling of a 3×4 *Chandra* ACIS-I mosaic survey in the ANEPD field (Krumpe *et al.* 2015; hereafter K15). Including additional ~ 50 ks of data from archive, we cover the field with exposure times ranging from ~ 40 – 80 ks. The source catalog and the first analysis of 457 X-ray sources is presented in K15.

In K15, (see Fig. 2 *left*), we compare the observed X-ray (2–7 keV) luminosity ($L_{\text{OBS},2-7\text{keV}}$, i.e. luminosity calculated without K-correction or absorption correction) and the AGN component of the IR luminosity $L_{\text{IR,AGN}}$ obtained from SED fitting using an updated version of the Hanami *et al.* (2012)'s procedure. By this comparison, we selected 28 strong Compton-thick AGN (CTAGN) candidates, i.e., AGNs with a line of sight column density of $N_{\text{H}} > 10^{24} [\text{cm}^{-2}]$.

The CTAGNs are characterized by a large equivalent width of the Fe K α line ($EW \gtrsim 1$ keV). Using the CSTACK utility†, we have made a rest-frame stacking of the X-ray spectra of the 28 strong CT AGN candidates (Fig. 2 *right*), obtaining an equivalent width

† <http://lambic.astrosem.unam.mx/cstack>

of the Fe K α of $EW = 1.0 \pm 0.6$ keV. This suggests that a majority of these candidates are CTAGNs with possible contamination from non-CT AGNs.

4. Prospects for eROSITA/ART-XC observations

The spacecraft *Spectrum-RG*, which is planned to be launched in the near future (Merloni, this symposium), carries two instruments, eROSITA (sensitive in 0.2–10 keV) and ART-XC (5–30 keV). The plan of the mission is to perform 8 all-sky surveys over four years and the every great circle scan will go through the Ecliptic pole regions. *Spectrum-RG* will provide with us the best-matched dataset for our studies of highly obscured AGNs in the ~ 5.4 deg 2 ANEPW field, which is centered at the exact NEP. The combination of the ANEPW survey with the eROSITA dataset, we expect to probe a high luminosity - highly absorbed AGN population.

Using the current determination of the X-ray luminosity function of AGNs at $0.4 < z < 2$ (Miyaji *et al.* 2015), N_{H} function (Ueda *et al.* 2014), and the expected flux limit of eROSITA in the 2–10 keV band (Merloni *et al.* 2012), we expect to identify ~ 270 CTAGN/semi-CTAGN candidates using the method described above. The ART-XC instrument is sensitive in 5–30 keV, we expect to improve the distinction between non-CT AGNs and CT-AGNs by adding the ART-XC dataset.

5. Concluding Remarks

We are in the process of improving the investigation. The improvements include:

- Spectroscopic followup of ANEPD X-ray sources, IR-selected AGNs and and CTAGN candidates, using large telescopes including Gran Telescopio Canarias, Keck, and Large Binocular Telescope.
- We will use updated models for the AGN torus. These include the Clumpy Torus model (Nenkova *et al.* 2008) on the infrared side. An X-ray torus clumpy model that has the consistent geometrical configurations/parameter definitions as the Nenkova *et al.* (2008) model is being developed by a group at Kyoto University (Tanimoto *et al.*, Ogawa *et al.* this symposium). We will use these models for a consistent IR-X-ray modeling in selecting CT-AGNs.

TM is supported by UNAM-DGAPA PAPIIT (IN104216, IN111319) and CONACyT (252531). He thanks the conference organizers/NAOJ for a travel support.

References

- Ciesla, L., Charmandaris, V., Georgakakis, A., Bernhard, E., Mitchell, P. D., Buat, V., Elbaz, D., LeFloc'h, E., *et al.* 2015, *A&A*, 576, A10
 Hanami, H., Ishigaki, T., Fujishiro, N., Nakanishi, K., Miyaji, T., Krumpe, M., Umetsu, K., Ohyama, Y., *et al.* 2012, *PASJ*, 64, 70
 Kim, S. J., Lee, H. M., Matsuhara, H., Wada, T., Oyabu, S., Im, M., Jeon, Y., Kang, E., *et al.* 2012, *A&A*, 548, A29
 Krumpe, M., Miyaji, T., Brunner, H., Hanami, H., Ishigaki, T., Takagi, T., Markowitz, A. G., Goto, T., *et al.* 2015, *MNRAS*, 446, 911
 Matsuhara, H., Wada, T., Matsuura, S., Nakagawa, T., Kawada, M., Ohyama, Y., Pearson, C. P., Oyabu, S., *et al.* 2006, *PASJ*, 58, 673
 Merloni, A., Predehl, P., Becker, W., Böhringer, H., Boller, T., Brunner, H., Brusa, M., Dennerl, K., *et al.*, 2012, *eROSITA Science Book: Mapping the Structure of the Energetic Universe*, arXiv:1209.3114
 Miyaji, T., Hasinger, G., Salvato, M., Brusa, M., Cappelluti, N., Civano, F., Puccetti, S., Elvis, M., *et al.* 2015, *ApJ*, 804, 104

- Murata, K., Matsuhara, H., Wada, T., Arimatsu, K., Oi, N., Takagi, T., Oyabu, S., Goto, T., *et al.* 2013, *A&A*, 559, A132
Nenkova, M., Sirocky, M. M., Ivezić, Ž., & Elitzur, M. 2008, *ApJ*, 685, 147
Ueda, Y., Akiyama, M., Hasinger, G., Miyaji, T., & Watson, M. G. 2014, *ApJ*, 786, 104

Discussion

TRIANI: Is there any effect of inclination angle in the AGN SED in IR?

MIYAJI: Yes, there is. Especially, there is silicate absorption in the case of an edge-on view of the torus. We are investigating in detail the IR SED of tori including the angle dependence of the Nenkova “Clumpy Torus” model. Also on the X-ray side, we will revise the model using the new “X-clumpy” torus model, which has matching geometries and parameter definitions of the Nenkova model. This is under development by a group at Kyoto University and some results of its preliminary version of are presented in this conference (posters P36 by Tanimoto and P22 by Ogawa).